J Neurophysiol 103: 2664–2674, 2010.
First published February 17, 2010; doi:10.1152/jn.00733.2009.

Sensorimotor Locus of the Buildup Activity in Monkey Lateral Intraparietal Area Neurons

Joonkoo Park and Jun Zhang
Department of Psychology, University of Michigan, Ann Arbor, Michigan

Submitted 12 August 2009; accepted in final form 7 February 2010

Park J, Zhang J. Sensorimotor locus of the buildup activity in monkey lateral intraparietal area neurons. *J Neurophysiol* 103: 2664–2674, 2010. First published February 17, 2010; doi:10.1152/jn.00733.2009. A study in 2002 using a random-dot motion-discrimination paradigm showed that an information accumulation model with a threshold-crossing mechanism can account for activity of the lateral intraparietal area (LIP) neurons. Here, mathematical techniques were applied to the same dataset to quantitatively address the sensory versus motor representation of the neuronal activity during the time course of a trial. A technique based on Signal Detection Theory was applied to provide indices to quantify how neuronal firing activity is responsible for encoding the stimulus or selecting the response at the behavioral level. Additionally, a statistical model based on Poisson regression was used to provide an orthogonal decomposition of the neural activity into stimulus, response, and stimulus-response mapping components. The temporal dynamics of the sensorimotor locus of the LIP activity indicated that there is no stimulus-response mapping-specific neuronal firing activity throughout a trial; the neural activity toward the saccadic onset reflects the development of the motor representation, and the neural activity in the beginning of a trial contains little, if any, information about the sensory representation. Sensorimotor analysis on individual neurons also showed that the neuronal activation, as a population, represent pending saccadic direction and carry little information about the direction of the motion stimulus.

INTRODUCTION

The lateral intraparietal (LIP) area, a subdivision of the inferior parietal lobule and a part of the association cortex, has been implicated in various computations related to perceptual decision making. Namely, it has been linked to information processing that occurs between the registration of the visual sensory stimulus and the programming of eye movement. For instance, LIP activity is known to correlate with saccadic movements and their planning (Barash et al. 1991a; Bracewell et al. 1996; Dickinson et al. 2003; Mazzoni et al. 1996; Mountcastle et al. 1975; Platt and Glimcher 1997; Snyder et al. 1997), visual attention, saliency, and sensory information (Goldberg et al. 2002; Gottlieb and Goldberg 1999; Gottlieb et al. 1998; Robinson et al. 1978; Shadlen and Newsome 1996), subjective valuation or motivation (Platt and Glimcher 1999; Sugrue et al. 2004), and the transformation of visual information into an eye movement (Barash et al. 1991b; Oristaglio et al. 2006; Russ et al. 2006; Zhang and Barash 2004). Notwithstanding the possibility of different roles mediated by different subsets of LIP neurons (Colby et al. 1996), an emerging viewpoint is that the LIP functions by accumulating sensory evidence over time for the purpose of generating a perceptual decision (Huk and Shadlen 2005; Mazurek et al. 2003; Roitman and Shadlen 2002; Shadlen and Newsome 2001).

Roitman and Shadlen (2002) tested this hypothesis using a random-dot motion stimulus and examined the neuronal activity of monkeys engaged in a two-alternative forced-choice reaction time task (Fig. 1*A*). Their results showed that, while the perceptual decision was being formed, the LIP firing rate built up during each trial up until the time of initiation of a behavioral response, and the rate of such "buildup" was monotonically related to the stimulus strength as controlled by the experimenter. This study supported the idea that perceptual decisions, as implemented by LIP neurons, can be modeled as a sequential sampling process with threshold-crossing decision mechanism—the animal continuously samples environmental input and responds as soon as the accumulated evidence in favor of one hypothesis (against the other alternative hypothesis) exceeds a preset threshold (see review by Shadlen and Gold 2004; Smith and Ratcliff 2004). Build-up activity had been previously found in the frontal eye field (Hanes and Schall 1996) and the superior colliculus (Basso and Wurtz 1997; Munoz and Wurtz 1995).

Previous analyses on LIP activity showed signal strength–dependent accumulation of the neuronal activity from stimulus onset up until response initiation of given trials. Here, two novel mathematical techniques allow us to analyze the same data in terms of their sensorimotor locus, which reflects the quantification of the relative contributions of sensory and motor representations, of the neuronal activity during the time course of a trial. In particular, for a simple task with two alternative stimulus directions and two alternative response directions, the pattern of correlation between the stimulus (or response) and the neural activity recorded on a trial-by-trial basis can be used to determine whether a neuron is performing stimulus encoding, response initiation, or the mapping between the two during a task (Zhang et al. 1997a,b). When neuronal activity is analyzed across the ensemble of trials (including those trials where the animal makes a behavioral error), a "predecision" or sensory neuron is one whose activity correlates better with stimulus categories than with response categories; the opposite should be true for a "postdecision" or motor neuron.

Previous analysis of 0% motion coherence and error trials (Roitman and Shadlen 2002) and other studies (Shadlen and Newsome 1996, 2001) has suggested that LIP activity primarily reflects response initiation rather than stimulus encoding. However, it is not clear whether the LIP neuronal activity during the buildup process entirely represents response initiation or if there is any stimulus encoding or stimulus-response mapping aspect during this process.

Address for reprint requests and other correspondence: J. Zhang, Dept. of Psychology, Univ. of Michigan, 530 Church St., Ann Arbor, MI 48109 (E-mail: junz@umich.edu).

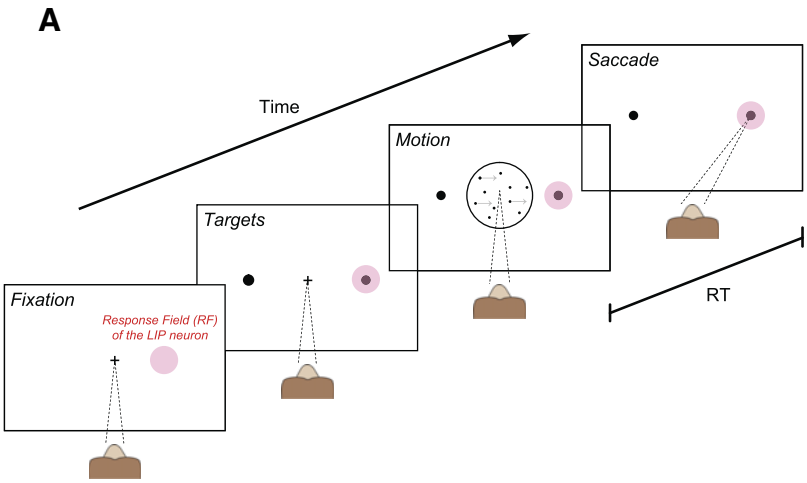

B

		Stimulus (Motion) Direction	
		Towards RF	Opposite of RF
Response (Saccade) Direction	Towards RF	Trial Type *S1R1*	Trial Type *S2R1*
	Opposite of RF	Trial Type *S1R2*	Trial Type *S2R2*

FIG. 1. Experimental paradigm with possible trial types. *A*: monkeys discriminated the direction of motion of a random-dot display in which a portion of the dots move randomly and the remaining dots move coherently either toward the response field (RF) or the opposite hemifield of a particular lateral intraparietal area (LIP) neuron. The direction and strength of coherent motion changes from trial to trial; the period from its onset to the behavioral saccadic movement is the reaction time. Adapted from Fig. 2*A* of Roitman and Shadlen (2002). *B*: the 4 different trial types. Trial types S1R1 and S1R2 share same stimulus direction (i.e., dots toward T1); so do trial types S2R1 and S2R2 (i.e., dots toward T2). Likewise, trial types S1R1 and S2R1 share the same behavioral response (i.e., saccade toward T1); so do trial types S1R2 and S2R2 (i.e., saccade toward T2). Note that trial types S1R1 and S2R2 are correct trials, and trial types S1R2 and S2R1 are incorrect trials.

In this study, we perform a refined analysis of the data presented in Roitman and Shadlen (2002) to quantitatively determine the neural sensorimotor locus and its possible transformation during the progression of a trial. A mathematical technique based on Signal Detection Theory (SDT) (Zhang et al. 1997a) and a statistical model incorporating orthogonal decomposition of neuronal activity (Zhang et al. 1997b) are independently applied to identify the sensory/motor/sensory-motor mapping aspect of neuronal coding for this random-dot motion discrimination task. Both analyses take advantage of incorrect trials (when motion strength is low) in defining the sensorimotor locus of the cell or cell population through comparing their firing activity in correct and incorrect trials. By incorporating incorrect trials in addition to correct ones, these analyses make it possible to disentangle the monkey's perceptual processing from its response preparation in interpreting the functional role of neuronal activities along the stimulus-response pathway. By comparing neural activity in trials where the animal decides to make saccades to one or the other direction (regardless of the stimulus direction) and in trials where the dots move to one or the other direction (regardless of the saccadic direction), these analyses enable quantitative assessment of the temporal dynamics of the transformation of sensorimotor representation of LIP neuronal activity during a perceptual decision making task.

METHODS

Participants and task procedures

The experimental procedure of Roitman and Shadlen (2002), whose data we analyzed, is briefly described here. Monkeys performed a two-alternative forced-choice task using random-dot motion stimuli (Fig. 1*A*). A trial began when the animal fixated at the central fixation point, after which two choice targets appeared simultaneously. One of the targets was located in the response field (RF) of the neuron (T1) and the other in the opposite hemifield (T2). After a variable interval, the random-dot motion stimulus appeared in the center with a net direction of motion toward either choice target. With the onset of the stimulus, the monkey's task was to judge the net direction of motion and indicate its decision by making a saccade toward the corresponding target. The monkey was free to indicate the choice at any time once the random-dot motion started. There were six motion strength levels (0, 3.2, 6.4, 12.8, 25.6, and 51.2%, indicating the percentage of dots moving coherently amid dots moving in random directions), and both the direction and strength of motion were chosen randomly on each trial. The period from the onset of the stimulus to saccade initiation is referred to as the reaction time (RT). Spike trains from single unit recording were subject to either peristimulus analysis where individual trials are time-locked to stimulus onset or periresponse analysis where individual trials are time-locked to response-onset—the two analyses yield non-identical results because RTs are not constant across the trials.

Roitman and Shadlen (2002) recorded single-unit activity from the neurons in area LIP of two female rhesus monkeys. The neurons were selected according to anatomical and physiological criteria. That is, a memory-guided saccade task was used to select neurons in area LIP that were active during saccade planning. Following this method, they identified a total of 54 LIP neurons (across 2 monkeys) with sustained response during the delay period when the random-dot motion stimulus was delivered to its response field (RF). The spike trains were available from 100 ms before stimulus onset to 200 ms after response onset in each trial.

The monkeys made very few errors under the conditions when the motion strength was 12.8% (70 incorrect trials of 1,033 total trials), 25.6% (5 incorrect trials of 1,026 total trials), and 51.2% (0 incorrect trials of 1,028 total trials). Our proposed analyses require a sufficient number of error trials (Zhang et al. 1997a); therefore these conditions were excluded from further analysis and we only make use of the data from motion strengths of 3.2% (368 incorrect trials of 1,028 total trials) and 6.4% (229 incorrect trials of 1,025 total trials).

Spike count and firing rate estimation

Peristimulus and periresponse spike trains were binned at every 20 ms to derive spike counts and firing probabilities at each time bin for each trial. The inverse of the firing probability, while taking the size of the bin into account, was considered as an estimate of the underlying firing rate at each 20 ms bin. The estimated firing rate from the correct trials reproduced the original results (Fig. 2*A*; cf. with Fig. 7 in Roitman and Shadlen 2002). The estimated firing rate from the incorrect trials in 3.2 and 6.4% motion coherence conditions also reproduced the original results (Fig. 2, *B* and *C*; cf. with Fig. 11 in Roitman and Shadlen 2002). The peristimulus and periresponse spike counts at each bin were used in the following mathematical techniques. In this analysis, peristimulus analysis included spikes from 100 ms before stimulus onset up to the response onset for each trial, and periresponse analysis included spikes from stimulus onset to 200 ms after response onset for each trial.

SDT-based analysis

The SDT-based analysis provides discriminability values to quantify how neuronal firing activity serves for encoding the stimulus or for selecting the response at the behavioral level. It provides an index for quantitatively specifying the locus of the neuronal activity along the sensorimotor continuum.

The spike count data for all trials were first categorized into the four possible trial types (Fig. 1*B*). The number of trials under each trial type is denoted N_{S1R1}, N_{S1R2}, N_{S2R1}, and N_{S2R2} in the rest of the paper. For each time bin (under both peristimulus and periresponse spike count data), trial type–specific spike histograms were constructed (see Fig. 3, four colored histograms). These histograms show the number of trials of a certain trial type (ordinate) that has a certain spike count (abscissa). These four histograms were pairwise combined to produce stimulus-sorted or response-sorted histograms (gray histograms) representing the conditional distribution of neuronal spike-rate according to stimulus or response categories, respectively. To illustrate, the combination of spike histograms of trial type S1R1 and trial type S1R2 yields the spike histogram for stimulus direction toward T1, and the combination of spike histograms of trial type S2R1 and trial type S2R2 yields the spike histogram for stimulus direction toward T2. After these stimulus-sorted spike-rate histograms are properly normalized (so that the area under each distribution sums to 1), they represent estimates of the probability density function of spike rates given the stimulus direction regardless of the monkey's response direction. Because correct trials outweigh incorrect trials, the resulting spike histograms may more closely resemble correct trial types than incorrect trial types. This approach effectively gives equal weight to each trial of all four trial types resulting in being probability distributions of the spike activity conditioned on the stimulus classification while being unconditional on the response categories. Analogously, response-sorted spike-rate histogram can be constructed from combining trial type S1R1 with trial type S2R1 and from combining trial type S1R2 with trial type S2R2.

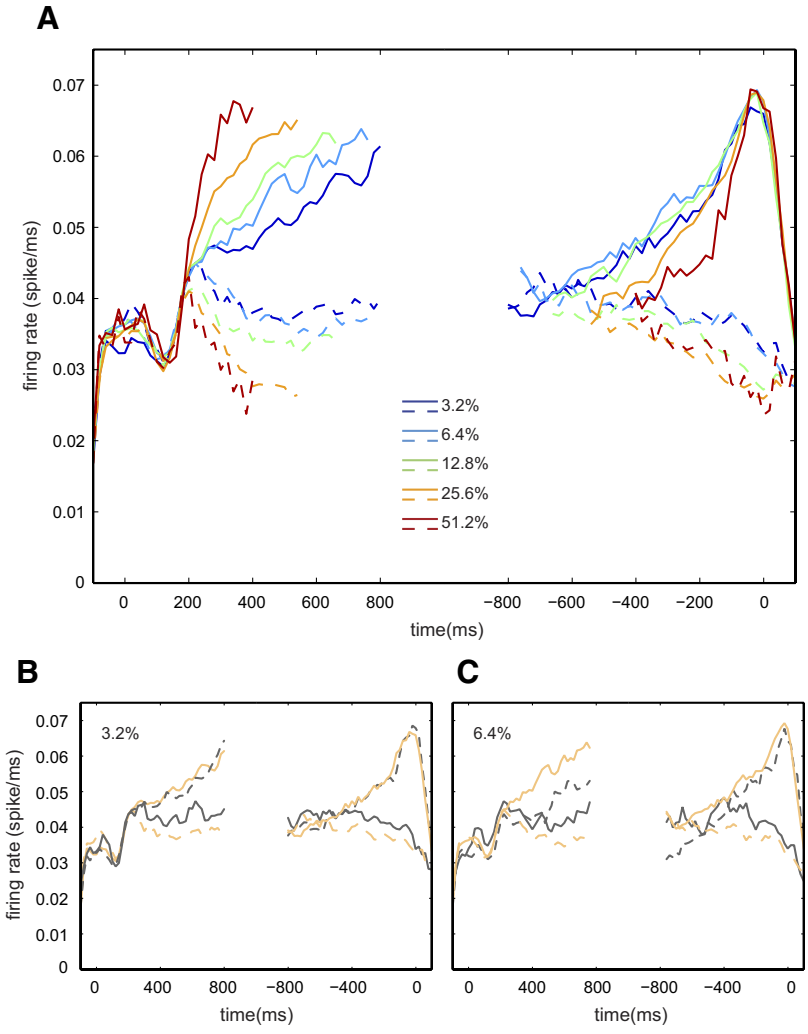

FIG. 2. Time course of LIP buildup activity. *A*: neuronal firing rates estimated from spike counts from the full dataset for each 20-ms bin grouped by motion strength and saccadic direction indicated by color and line type, respectively. Solid lines indicate saccadic direction toward T1 and dashed lines indicate saccadic direction toward T2. Only correct trials are included in this graph. *B*: comparison of neuronal firing rates during the error trials in the 3.2% motion coherence condition. *C*: comparison of neuronal firing rates during the error trials in the 6.4% motion coherence condition. Colored lines in *B* and *C* are reproduction of the 2 correct trials (S1R1 for solid and S2R2 for dashed) in *A*, and gray lines indicate the firing rates for the 2 incorrect trials (S1R2 for solid and S2R1 for dashed). *Left*: peristimulus analysis, which spans from 100 ms before stimulus onset until median reaction time (mRT). *Right*: response-locked analysis from –mRT to 100 ms after response initiation. The plots were smoothed using a 60-ms running mean.

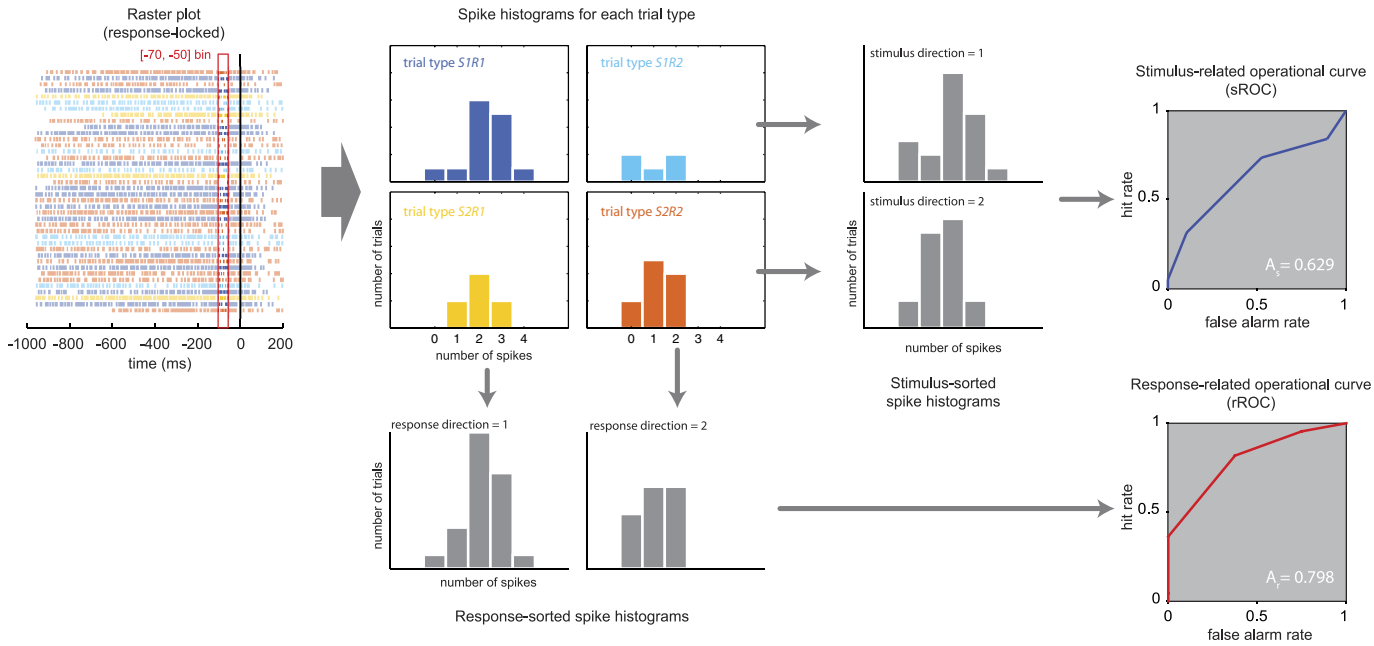

FIG. 3. Analysis based on signal detection theory is described using a dataset from a peririesponse spike train of a particular neuron (cell 1618). This particular figure shows the derivation of sROC and rROC at a particular time bin [−70 ms, −50 ms]. Four types of spike histograms are derived from this time bin (colored histograms). After normalization, the stimulus-sorted spike-rate histograms generate sROC, and the response-sorted spike-rate histograms generate rROC. The area under these curves are used to yield a sensorimotor index λ for the given time point (Zhang et al. 1997a). Color coding conventions for the trial types are the same as Fig. 1.

Once the stimulus-sorted (response-sorted) spike-rate histograms are constructed, a stimulus-referenced (response-referenced) operating curve, or sROC (rROC, which differs from the "sender operational characteristic" of the SOC curve of Newsome et al. 1989), can be obtained by standard procedures (Fig. 3, the 2 boxes on the *right*). The area under an sROC curve (A_s) is a measure of the discriminability of the stimulus direction given the neuronal firing rates; similarly, the area under an rROC curve (A_r) is a measure of the discriminability of the response direction given the neuronal firing rates. It is important to determine whether A_s or A_r is reliably different from 0.5, a value which implies that the neural activity cannot discriminate either the two stimulus or the two response directions. To do so, confidence intervals for A_s and A_r at each time point are constructed using a bootstrap resampling method. For each bootstrap sample, spike trains, trial types, and behavioral performance from individual trials are resampled with replacement, and the above procedure was performed. The resulting metrics were rank ordered for each time bin, and the interval between the 0.5 and the 99.5 percentiles of the bootstrap distribution was identified as the 99% CI.

To derive a single measure of sensorimotor index, A_s and A_r are first transformed into a stimulus-related discriminant [$\Sigma_s = 2(A_s - 0.5)$] and a response-related discriminant [$\Sigma_r = 2(A_r - 0.5)$], which range from −1.0 to 1.0. The relative magnitudes of Σ_s and Σ_r reflect the reliability in predicting stimulus or response categories from the neuronal spike rate. Similarly, the discriminant for the two kinds of correct trials, Σ_o, can be calculated from the area under an operational curve generated from the distribution of the two correct trials, A_o. The sensorimotor index (λ) can be calculated using variables referenced to stimulus as

$$\lambda = \frac{\Sigma_o - \Sigma_s}{\varepsilon_s \Sigma_o} \qquad (1)$$

or can be calculated (Zhang et al. 1997a) using variables referenced to response as

$$1 - \lambda = \frac{\Sigma_o - \Sigma_r}{\varepsilon_r \Sigma_o} \qquad (2)$$

where ε_s [defined by $N_{S1R2}/(N_{S1R1} + N_{S1R2}) + N_{S2R1}/(N_{S2R1} + N_{S2R2})$] and ε_r [defined by $N_{S2R1}/(N_{S1R1} + N_{S2R1}) + N_{S1R2}/(N_{S1R2} + N_{S2R2})$] are stimulus- and response-referenced error rates, respectively. Assuming that a symmetric mixture hypothesis holds (see below), Σ_o may be eliminated from these two equations to yield

$$\lambda = \frac{(\Sigma_r - \Sigma_s) + \varepsilon_r \Sigma_s}{\varepsilon_r \Sigma_s + \varepsilon_s \Sigma_r} \qquad (3)$$

The value λ is a measure that characterizes the role of a neuron or a population of neurons in the processing continuum between sensory input and response output, with λ = 0 corresponding to a pure sensory neuron and λ = 1 a pure motor neuron. When the neuron has a better discriminability for the correct trials than for the incorrect trials (i.e., when the spike histograms for the trial types S1R1 and S2R2 are more separated than that for the trial types S1R2 and S2R1), λ lies in the range [0, 1]. However, λ lies outside the range [0, 1] when the neuron has a better discriminability for the incorrect trials. The transformation $\lambda \rightarrow \lambda/(2\lambda - 1)$ allows us to compute λ within [0, 1], regardless of whether the neuron better discriminate the correct trials or the incorrect trials.

In deriving the sensorimotor index as a unitary measure of sensorimotor locus, it is assumed that neuronal activity on the incorrect trials (trial types S1R2 and S2R1) are symmetric mixtures of neuronal activity on correct trials (trial types S1R1 and S2R2) or vice versa. This so-called "symmetric mixture" hypothesis asserts that the neuronal activities on the correct trials and incorrect trials are balanced, which should be true for neurons along the sensorimotor arc (i.e., not encoding a stimulus-response mapping rule or reward). This hypothesis makes certain predictions about the discriminant values and the error rates, which can be empirically tested. Specifically, one can evaluate the expressions of $(\Sigma_O - \Sigma_s)/\varepsilon_s\Sigma_O$ and $(\Sigma_O - \Sigma_r)/\varepsilon_r\Sigma_O$, and check whether the results sum to 1.0 (which they should if the

symmetric mixture hypothesis is satisfied). Such a test was performed on the full dataset, for each time bin throughout a trial (Fig. 4), and the results were confirmed the prediction of the symmetric mixture hypothesis.

Cell-by-cell analysis of the sensorimotor index

SDT-based analysis was performed on each neuron, and each neuron's sensorimotor index (λ) was estimated at the beginning and at the end of a trial. First, each neuron's peristimulus and periresponse λ values were computed (Fig. 6 shows such values for 2 representative neurons). Then, the time course of the peristimulus analysis from stimulus onset to mRT (median reaction time) of the particular neuron was divided into three equal-length intervals. Likewise, the time course of the periresponse analysis from –mRT (of the particular neuron) to motion onset was divided into three equal-length intervals. Task-related neuronal activity does not reach LIP until ~200 ms after stimulus onset (Britten et al. 1992; Roitman and Shadlen 2002) and the task-relatedness of the neuronal activity (−2LL in Fig. 7) also increases after about one-third mRT. We therefore computed the mean λ value during the second time interval [1/3 × mRT, 2/3 × mRT] of the peristimulus analysis to represent the sensorimotor index near stimulus onset. The mean λ value during the last time interval [−1/3 × mRT, 0] of the periresponse analysis was computed to represent the sensorimotor index near response onset. Because the mRTs for the full dataset across all trials were 814.5 ms and 762 ms for 3.2 and 6.4% conditions, respectively, we expected that an interval with a length of one third of mRT would be a reasonable time frame to capture sensorimotor transformation near the beginning (excluding the first 200 ms) and at the end of a trial. Note that λ was not computed for the neurons with no error trials.

Orthogonal decomposition of neuronal activity

A statistical model incorporating orthogonal decomposition of variances in the dependent measure (i.e., neuronal firing activity) provides another way to quantify the sensory and motor representations of neuronal activity with a slightly different perspective on the dataset. To be specific, we fitted three orthogonal contrasts of neuronal activities (stimulus-related, response-related, and stimulus-response mapping-related) into spike counts at each time bin using a Poisson regression model. The approach is similar to the locus analysis (Zhang et al. 1997b) except that this statistical model treats spike counts as random variables and thus allows statistical inference. This approach provides quantitative assessments of the extent to which the spike count encodes stimulus direction, response direction, or the stimulus-response mapping rule. In addition, this approach is capable of quantifying overall task-relatedness of the spike activity.

A Poisson regression model was constructed for each 20 ms bin with the spike count as a dependent measure and three predictors with an intercept as independent variables. The first predictor (*S*) was a contrast code that had 1s for trials with stimulus direction toward T1 and −1s for stimulus direction toward T2. The second predictor (*R*) was a contrast code that had 1s for trials with response direction toward T1 and −1s for response direction toward T2. Finally, the third predictor (*SR*) was a contrast code that had 1s for correct trials and −1s for incorrect trials. These three contrasts are orthogonal and formed the basis of the locus analysis (Zhang et al. 1997b) in which *X, Y, Z* are computed from the firing activities of the four trials types V_{S1R1}, V_{S1R2}, V_{S2R1}, and V_{S2R2} via

$$X = V_{S1R1} + V_{S1R2} - V_{S2R1} - V_{S2R2}$$

$$Y = V_{S1R1} - V_{S1R2} + V_{S2R1} - V_{S2R2}$$

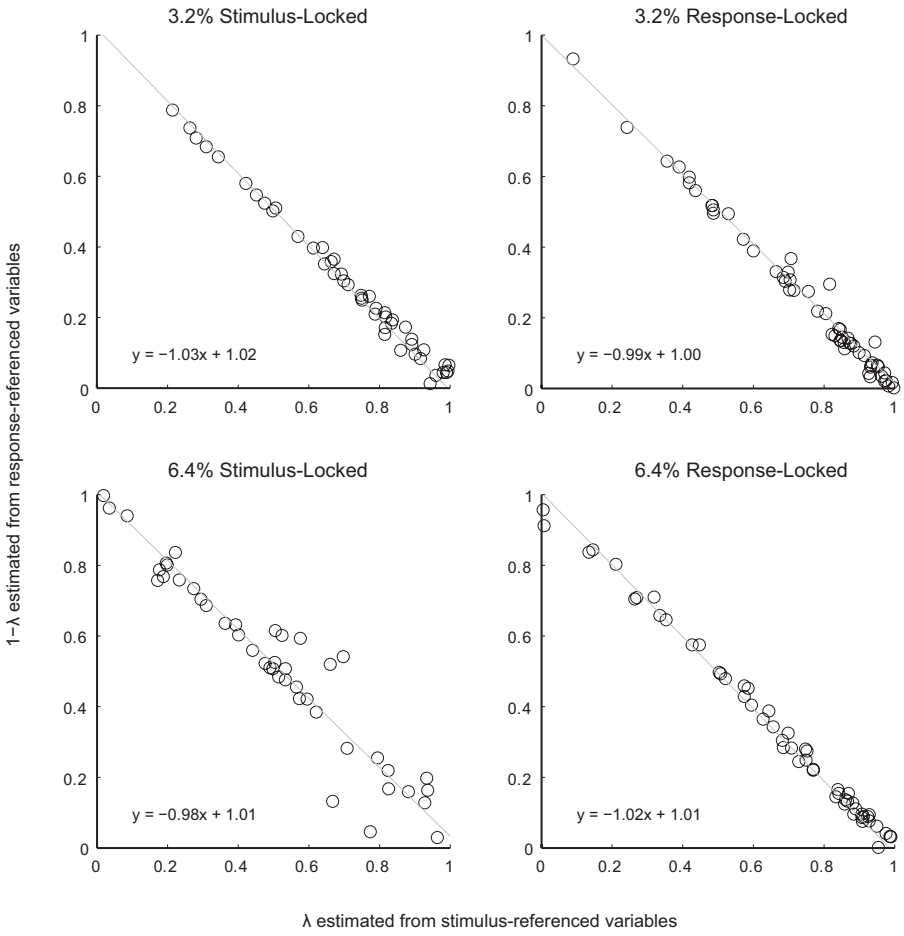

FIG. 4. Test of the symmetric mixture hypothesis. Each graph shows the scatter plot of λ estimated from the stimulus-referenced variables (*Eq. 1*) and 1 − λ estimated from the response-referenced variables (*Eq. 2*) under different motion strengths (3.2 and 6.4%) and peristimulus and periresponse spike counts. Each circle in the plot represents a single time point in the overall time course of a trial in the full dataset analysis, and a straight line is fitted with ordinary least squares methods yielding a slope and intercept. The symmetric mixture hypothesis predicts that the sum of these 2 estimates equal 1.0 (negative diagonal line).

$$Z = V_{S1R1} - V_{S1R2} - V_{S2R1} + V_{S2R2}$$

The mean of the spike count at each time bin was plotted against the variance of the spike count, and a straight line was fitted with ordinary least squares method to assess the relationship between the mean and the variance of the dependent measure (Fig. 8; mean and variance are the same under Poisson distribution). β estimates of the contrast codes that represent stimulus, response, and stimulus-response mapping components are computed at each bin (Fig. 9). Moreover, 99% CIs for the stimulus component (from 200 ms after the onset of motion in the peristimulus spike train) and the response component (until the saccadic onset in the periresponse spike train) were assessed. In addition, the difference of the deviance for the full model (with all predictors and a constant) and the constant model (with only a constant) was computed. This measure (-2LL; -2 multiplied by the difference between the 2 log-likelihoods) approximates to a χ^2 distribution with 3 degrees of freedom and assesses whether the spike activity contains any information related to the three orthogonal predictors, which may be interpreted as a measure of task-relatedness of the neuronal activity.

RESULTS

The dataset being analyzed here is from Roitman and Shadlen (2002), courtesy of Dr. Michael Shadlen (http://www.shadlen.org/Science/Data). In that study, neuronal firing activity was recorded from 54 neurons in LIP from two rhesus monkeys performing a two-alternative forced-choice reaction time task using random-dot motion as the stimulus and eye movement as the response (Fig. 1). The data from trials with motion strengths (percentage of dots moving coherently in one direction) 3.2 and 6.4% were used for our reanalysis, because both analyses require a sufficient number of incorrect trials. In the 3.2% condition, $N_{S1R1} = 337$, $N_{S1R2} = 175$, $N_{S2R1} = 193$, and $N_{S2R2} = 323$. In the 6.4% condition, $N_{S1R1} = 409$, $N_{S1R2} = 104$, $N_{S2R1} = 125$, and $N_{S2R2} = 387$.

From SDT-based analysis

The relationship between neuronal firing activity and stimulus and/or response was characterized by computing how activity at the neuronal level would discriminate stimulus categories delivered to the animal or response categories intended and eventually performed by the animal. The discriminability values for stimulus identification and response preparation were respectively operationalized by the area under the stimulus-referenced operating characteristic curve (A_s) and the area under the response-referenced operating characteristic curve (A_r) (Fig. 3; see METHODS). From the two respective areas, an index λ, ranging [0, 1], was constructed such that the pattern of neuronal activity can be placed along a sensorimotor continuum, with 0 indicating pure sensory locus and 1 indicating a pure motor locus. The symmetric mixture hypothesis was tested by plotting λ estimated from stimulus-referenced variables and $1 - \lambda$ from response-referenced variables (see METHODS). Because these two values sum to 1 for all cases (Fig. 4), we may assume that neuronal activity on error trials is a linear mixture of neuronal activity on correct trials and that neurons are not encoding stimulus-response mapping rule.

Figure 5 shows the results of the SDT-based analysis of the full dataset under two motion strengths. The *top* and *bottom panels* in Fig. 5*A* show the evolution of A_s, A_r, and λ under the 3.2% condition and the two panels in Fig. 5*B* likewise show the evolution of A_s, A_r, and λ under the 6.4% condition. In both conditions, neural activity discriminated well the response direction toward the end of a trial as indicated by large A_r. In the 3.2% condition, there was no indication of stimulus direction discriminability throughout a trial. In the 6.4% condition, on the other hand, neural activity was better than chance (0.5) at discriminating stimulus direction toward the end of a trial. It should be noted, however, that A_r was generally greater than A_s throughout, which indicates that the spike activity primarily encoded the impending motor response. The sensorimotor

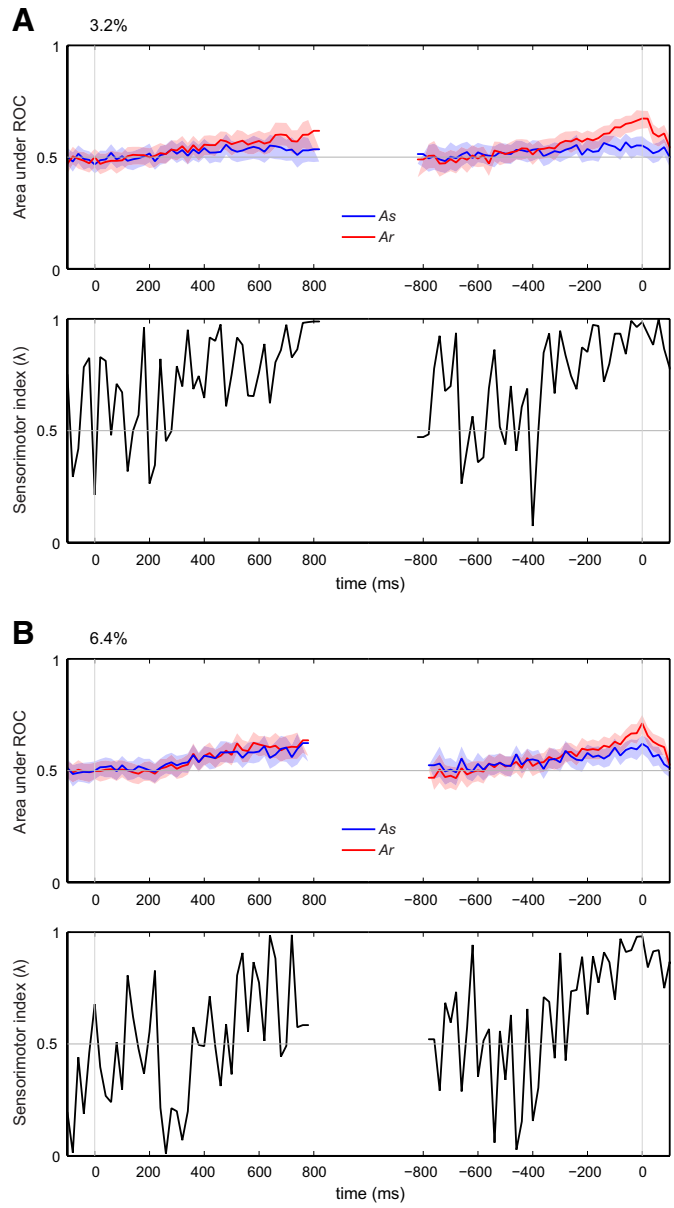

FIG. 5. Temporal dynamics of the areas under sROC (A_s) and rROC (A_r) and the sensorimotor index of the full dataset from the 3.2% condition (*A*) and the 6.4% condition (*B*). For each panel, the *top panel* shows the discriminability of stimulus and response directions given the neuronal spike activity, and the *bottom panel* shows the evolution of sensorimotor index (λ) as calculated from A_s, A_r, and the behavioral error rates. $\lambda = 0$ means a pure sensory locus, whereas $\lambda = 1$ means a pure motor locus in the sensorimotor continuum. The plots were smoothed using a 60-ms running average. The 99% CIs for A_s and A_r are shown in partly transparent shaded background. The horizontal axis uses the same conventions as in Fig. 2.

index (λ) summarizes this pattern. There was high level of fluctuations in λ near stimulus onset. Assuming that LIP activity in the initial ~200 ms is task independent (Britten et al. 1992; Roitman and Shadlen 2002 see Fig. 2 as well), it is natural to expect that the fluctuations in λ in this time frame were caused by random noise unrelated to the task. Therefore to assess whether there is any evidence for sensory encoding at the beginning of a trial, we focused on the time frame in between 200 and 400 ms after stimulus onset. There is yet no evidence for sensory encoding in this time frame as indicated by highly fluctuating λ values and large confidence bands for both the 3.2 and 6.4% conditions. This was in stark contrast with the pattern of λ values near response onset, where λ reached closer to 1 with tighter confidence bands for both the 3.2 and 6.4% conditions. This result suggests that LIP activity reflects the direction of the impending motor response near the end of a trial.

In the 6.4% condition, λ values were particularly low between 200 and 400 ms after stimulus onset. This pattern was also reflected in the data points in the lower ranges of the abscissa in the plots for the symmetric mixture hypothesis (Fig. 4). We suspect that this low λ is a result of random fluctuations rather than an indication of a purely sensory neuron, because the magnitudes of both A_s and A_r were close to 0.5 (in fact, their confidence bands included 0.5) and because the confidence band for λ was large. However, it is interesting to observe the simultaneous rise of both A_s and A_r in the next 200 ms with equal magnitude, indicative of a sensorimotor locus around 0.5.

In their original analysis, Roitman and Shadlen (2002) excluded any activity within 100 ms of response onset for the peristimulus analysis to reduce any presaccadic enhancement. Likewise, they excluded any activity within 200 ms of motion onset for the periresponse analysis to reduce any activity associated with stimulus onset. We performed the SDT-based analysis again while, this time, excluding the neuronal activity near stimulus and response onset as was done in the original study. The results were not qualitatively different from the initial results (Supplemental Fig. S1)[1]; for example, A_r was greater than or equal to A_s in the peristimulus analysis. This further suggests that the patterns we observed in the SDT-based analysis did not depend on activity associated with presaccadic enhancement or task-irrelevant activity near motion onset.

From cell-by-cell sensorimotor index analysis

To appreciate the wide variability of individual LIP neurons, peristimulus and periresponse temporal dynamics of the sensorimotor index (λ) were calculated for each neuron. Results from two representative neurons are shown in Fig. 6, and the mean λ near the stimulus onset and near the response onset was computed for each neuron as shown in Fig. 7. We first tested whether the sensorimotor role of each neuron remained relatively stable as a function of motion coherence. In other words, stability means that a neuron with a higher λ value in the 3.2% condition will also have a higher λ value in the 6.4% condition and vice versa. In fact, the λ values between the two conditions were significantly correlated ($r = 0.305$, $p = 0.031$ for λ values near stimulus onset; $r = 0.377$, $p = 0.007$ for λ values near response onset), indicating a relatively stable sensorimotor role across all neurons.

Cell-by-cell scatter plots of the λ values (Fig. 7) confirm the findings from the full dataset—neurons mostly represent response-related activity ($\lambda > 0.5$) rather than stimulus-related activity ($\lambda < 0.5$), especially near the response onset. A *t*-test on the λ values near response onset indicated that the mean λ across neurons was significantly above 0.5 [$t(53) = 5.146$, $p < 0.001$ for 3.2%; $t(49) = 6.267$, $p < 0.001$ for 6.4%]. The mean

[1] The online version of this article contains supplemental data.

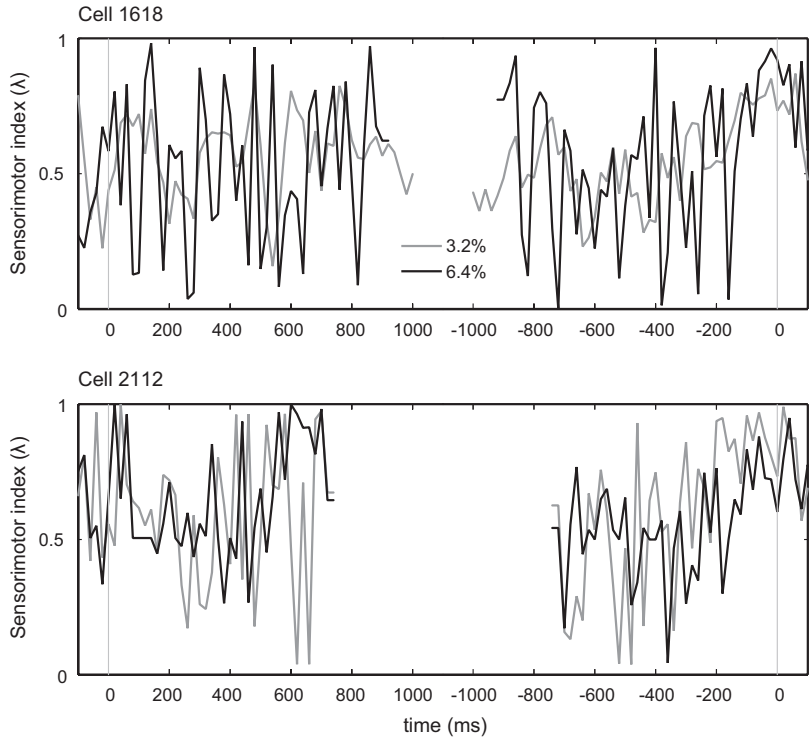

FIG. 6. The sensorimotor index during a trial for 2 individual neurons (cell 1618 and cell 2112). The plots were smoothed using a 60-ms running average. For cell 1618, mean of λ near stimulus onset was 0.576 ± 0.0686 and 0.488 ± 0.0741 (SD) for 3.2 and 6.4% conditions, respectively. Mean of λ near response onset was 0.656 ± 0.0469 and 0.631 ± 0.0749 for 3.2 and 6.4% conditions, respectively. For cell 2112, mean of λ near stimulus onset was 0.458 ± 0.0835 and 0.528 ± 0.0574 for 3.2 and 6.4% conditions, respectively. Mean of λ near response onset was 0.821 ± 0.0381 and 0.656 ± 0.0428 for 3.2 and 6.4 conditions, respectively.

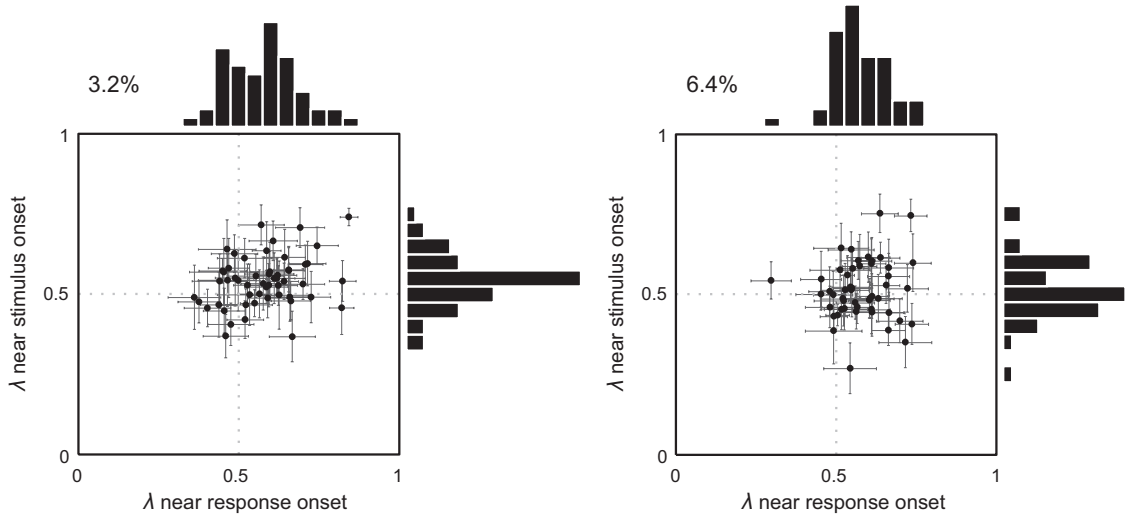

FIG. 7. Cell-by-cell computation of sensorimotor index (λ) at two time points during a trial for the 3.2% condition (*left*) and the 6.4% condition (*right*). Each dot represents a neuron, and its coordinate on the scatter plot indicates mean λ computed within a small time interval after stimulus onset (ordinate) and mean λ computed within a small time interval near response onset (abscissa). Error bar indicates SE. The histogram shows the distribution of the neurons along λ. Dotted line indicates λ = 0.5 to aid visualization.

λ values across neurons near stimulus onset was significantly above 0.5 in the 3.2% condition [$t(53) = 3.748$, $p < 0.001$] but not in the 6.4% condition [$t(49) = 1.043$, $p = 0.302$]. That more neurons represent $\lambda > 0.5$ in the 3.2% condition may be due to the long time interval in the computation of λ near stimulus onset, and hence the intrusion by the rise of the response-related activity. There were no apparent patterns indicating subdivisions of these neurons, although the noisiness of the λ values across neurons (i.e., wide distributions of the mean λ values), caused by low number of trials per neuron, may obscure the underlying structure.

In summary, the analyses provide quantitative assessments of the sensorimotor locus of the LIP activity as a trial progresses. The results corroborate the proposition that LIP activity primarily reflects the direction of the response near saccadic onset. They also suggest that there is a possibility that LIP activity may encode stimulus-related information to some extent after the stimulus onset, although it is not possible to precisely verify this using the current method.

From orthogonal contrasts analysis

Using orthogonal contrasts with spike count data in a Poisson regression, LIP activity was decomposed into three components: a stimulus component (*S*), a response component (*R*), and an SR mapping component (*S*-*R*). Scatter plots of the mean and variance of the spike counts (Fig. 8) confirmed that the spike counts follow Poisson distribution and allowed for further analysis. Figure 9 shows how coefficient estimates for each of the orthogonal components evolves as a trial progresses. Particularly, 99% CI for the stimulus and the response components were derived for the peristimulus and periresponse analyses, respectively. As expected, the spike counts were highly correlated with the motoric aspect in the periresponse analysis. The rapid increase of the response component suggests that the LIP build-up activity near saccadic onset is mainly driven by the preparation for response initiation. In the peristimulus analysis, the spike counts failed to be significantly associated with the stimulus component, although there was a trend for increasing β estimates for the stimulus component in the 6.4% condition between 250 and 500 ms after stimulus onset. Although we do not exclude the possibility of stimulus-related neuronal activity near the stimulus onset, we view the increase of the stimulus component in this time frame as mainly related to the increase in task-relatedness of the neuronal activity represented by −2LL in Fig. 7. At the same time, −2LL does not exceed 7.81 ($p < 0.05$; note that −2LL follows a χ^2 distribution with 3 degrees of freedom) nor 11.34 ($p < 0.01$) until 360 ms after stimulus onset, so the significance of the β estimates before this time point should be cautiously interpreted. It is also worth noting that there was no significant stimulus-response mapping component throughout a trial, which is consistent with our previous test of the symmetric mixture hypothesis.

DISCUSSION

In this study, we analyzed the information accumulation process in the LIP activity and examined the sensorimotor nature of the representation of information encoded by those LIP neurons on a trial-by-trial basis. Based on prior analyses of 0% motion coherence trials and error trials, there is little doubt that that LIP activity primarily reflects the direction of the motor response (Roitman and Shadlen 2002). This study provides a quantitative assessment on the sensorimotor locus of the LIP buildup activity during the time course of a trial. The SDT-based analysis provides a quantitative measure of sensorimotor locus of the neuron at each time point, and the Poisson regression model incorporating orthogonal decomposition of neuronal activity provides a quantitative assessment as to how the stimulus, response, and stimulus-response mapping components contribute to the spike activity.

The results show that the motoric representation (e.g., impending saccadic direction) of the LIP activity builds up and peaks at the saccadic onset. Near the saccadic onset, the discriminability of the response direction (A_r) peaks, sensorimotor index λ reaches 1, and the β estimate of the response component reaches its maximum. This pattern suggests that, at least in the later half time course of a trial, the neuronal activity

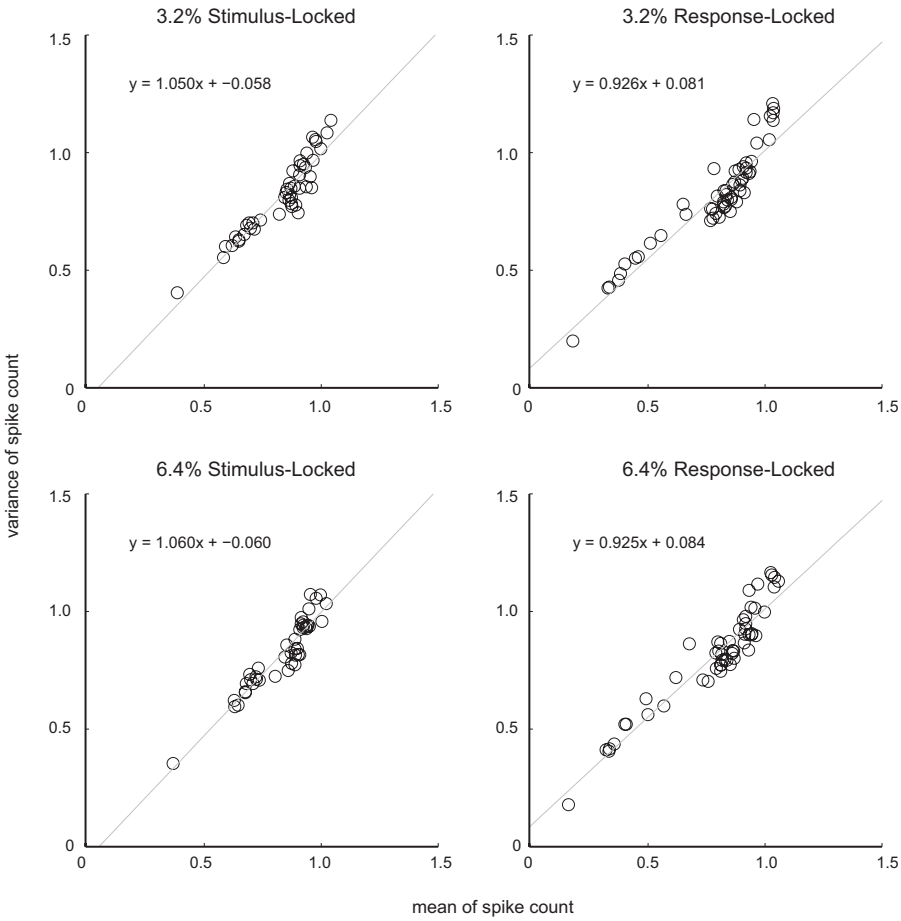

FIG. 8. Mean and variance plots for the spike count data. Each circle in the plot represents a single time point in the overall time course of a trial in the full dataset, and a straight line is fitted with ordinary least squares methods yielding a slope and intercept. Approximate equality of mean and variance of the spike counts suggests that the spike counts follow a Poisson distribution.

reflects the development of the motor plan, and it is consistent with the idea that LIP activity represents the direction of the response (Roitman and Shadlen 2002; Shadlen and Newsome 2001). What may be more interesting is the temporal dynamics of sensory representation in the beginning of a trial. Does the early part of the LIP buildup activity simply reflect the initial development of the motoric representation or does it also contain any sensory representation? The data suggest that there is no significant trend for stimulus-related neuronal activity in the beginning of a trial.

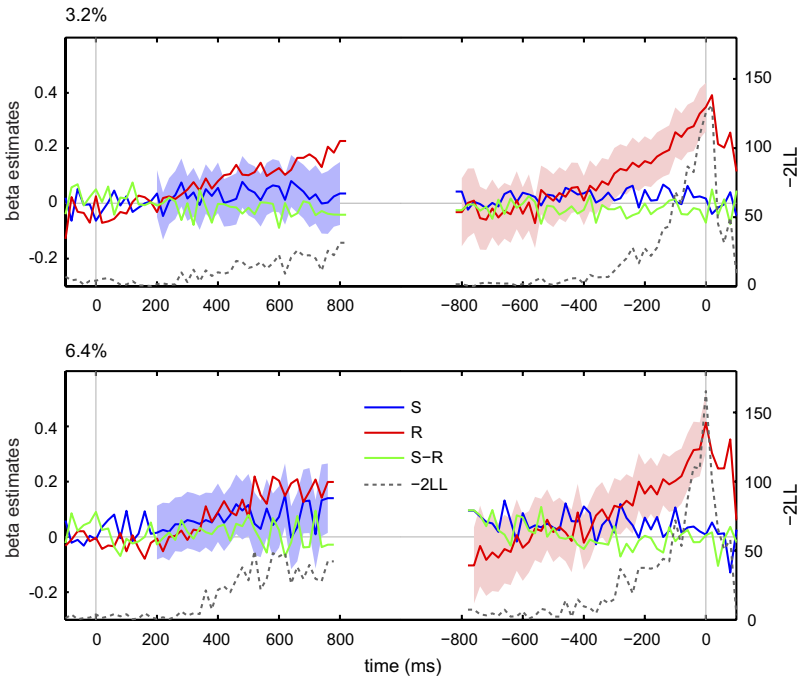

FIG. 9. Temporal dynamics of β estimates of orthogonal contrasts analysis for 3.2 and 6.4% conditions. β estimates of the stimulus (S), response (R), and stimulus-response mapping (S-R) components are represented in blue, red, and green lines, respectively (scale on the left ordinate). Dashed black lines represent, at each time point, values of −2LL, a measure of task-relatedness of the spike activity (scale on the right ordinate). Horizontal axis uses the same conventions as in Fig. 2; 99% CIs for S during [200 ms, mRT] and R during [−mRT, 0 ms] are filled with light blue and light red areas, respectively. The plots were smoothed using a 60-ms running average.

LIP is anatomically located in the sensorimotor network receiving input from the middle temporal area (MT) and providing output to the frontal eye field and the superior colliculi (Andersen et al. 1990, 1992). Neuronal activity in this area has been previous reported to be primarily associated with motor intention (Mazzoni et al. 1996; Snyder et al. 1997; Zhang and Barash 2000) or sensory attentive processing (Bisley and Goldberg 2003; Colby and Goldberg 1999; Gottlieb and Goldberg 1999). More recent studies suggested that the activity in this area contains both sensory- and motor-related aspects and even aspects of sensorimotor transformation (Buneo and Andersen 2006; Gottlieb et al. 2005; Zhang and Barash 2004). The results of this study cannot be directly compared with these other studies because of the different nature of the task—the "stimulus" in this study was a random dot motion centered at the fixation point rather than one of the targets located in the RF (or away from the RF) of the neuron. However, these findings that the buildup activity represents motor (but not sensory) information suggests that the neuronal activity in area LIP primarily reflects pending saccadic movement and carries little information about the encoding and processing evoked by the random dot motion stimulus.

It is possible that, at the beginning of a trial, noisy fluctuation of the functional components and sensorimotor indices (caused by relatively low firing rates) may have obscured the presence of a sensory component in LIP activity. However, a more likely interpretation is that, during the initial period of a trial, stimulus information needed for decision making has simply not reached LIP yet for this random-dot direction discrimination task. Mazurek et al. (2003) proposed a three-stage model for perceptual decision-making in which direction-selective MT neurons (stage 1) are driven by the motion stimulus in an antagonistic fashion (i.e., for both motion directions matching both the preferred and anti-preferred direction of an MT neuron) and then feed into LIP neurons (stage 2), which accumulate the MT inputs until a threshold is reached to trigger an eye movement downstream (stage 3). If MT neurons encode stimulus direction in this task (Britten et al. 1992; Newsome et al. 1989), it is natural to expect MT activity to show a pure sensory locus that precedes the buildup activity in LIP, which is shown here to carry a motoric representation. Under this interpretation, a monkey's perceptual decision is implemented by the MT-to-LIP synaptic connectivity, with MT implementing a predecision stimulus identification stage and LIP implementing a postdecision response selection stage, without the need for any intervening decision neuron—such dynamics for decision making under uncertainty is precisely what is prescribed by sequential sampling models. If MT neurons encode perceived stimulus direction in this task (Britten et al. 1996), a monkey's perceptual decision may be implemented by the MT neurons or even at the earlier stages of the visual processing. Further proof for such mechanisms for perceptual decision making would require performing sensorimotor analysis of the sort described in this report on simultaneously recorded MT and LIP neuronal activities.

ACKNOWLEDGMENTS

We thank M. Shadlen, who kindly made the data of Roitman and Shadlen (2002) available on-line.

GRANTS

This project is supported by Air Force Office of Scientific Research Grant FA9550-06-0298 awarded to the University of Michigan.

REFERENCES

Andersen RA, Asanuma C, Essick G, Siegel RM. Corticocortical connections of anatomically and physiologically defined subdivisions within the inferior parietal lobule. *J Comp Neurol* 296: 65–113, 1990.

Andersen RA, Brotchie PR, Mazzoni P. Evidence for the lateral intraparietal area as the parietal eye field. *Curr Opin Neurobiol* 2: 840–846, 1992.

Barash S, Bracewell RM, Fogassi L, Gnadt JW, Andersen RA. Saccade-related activity in the lateral intraparietal area. I. Temporal properties - comparison with area 7A. *J Neurophysiol* 1095–1108, 1991a.

Barash S, Bracewell RM, Fogassi L, Gnadt JW, Andersen RA. Saccade-related activity in the lateral intraparietal area. II. Spatial properties. *J Neurophysiol* 1109–1124, 1991b.

Basso MA, Wurtz RH. Modulation of neuronal activity by target uncertainty. *Nature* 121: 66–69, 1997.

Bisley JW, Goldberg ME. Neuronal activity in the lateral intraparietal area and spatial attention. *Science* 299: 81–86, 2003.

Bracewell RM, Mazzoni P, Barash S, Andersen RA. Motor intention activity in the macaque's lateral intraparietal area. II. Changes of motor plan. *J Neurophysiol* 76: 1457–1464, 1996.

Britten KH, Newsome WT, Shadlen MN, Celebrini S, Movshon JA. A relationship between behavioral choice and the visual responses of neurons in macaque MT. *Vis Neurosci* 13: 87–100, 1996.

Britten KH, Shadlen MN, Newsome WT, Movshon JA. The analysis of visual-motion—a comparison of neuronal and psychophysical performance. *J Neurosci* 12: 4745–4765, 1992.

Buneo CA, Andersen RA. The posterior parietal cortex: sensorimotor interface for the planning and online control of visually guided movements. *Neuropsychologia* 44: 2594–2606, 2006.

Colby CL, Duhamel JR, Goldberg ME. Visual, presaccadic, and cognitive activation of single neurons in monkey lateral intraparietal area. *J Neurophysiol* 76: 2841–2852, 1996.

Colby CL, Goldberg ME. Space and attention in parietal cortex. *Annu Rev Neurosci* 22: 319–349, 1999.

Dickinson AR, Calton JL, Snyder LH. Nonspatial saccade-specific activation in area LIP of monkey parietal cortex. *J Neurophysiol* 90: 2460–2464, 2003.

Goldberg ME, Bisley J, Powell KD, Gottlieb J, Kusunoki M. The role of the lateral intraparietal area of the monkey in the generation of saccades and visuospatial attention. *Ann N Y Acad Sci* 956: 205–215, 2002.

Gottlieb J, Goldberg ME. Activity of neurons in the lateral intraparietal area of the monkey during an antisaccade task. *Nat Neurosci* 2: 906–912, 1999.

Gottlieb JP, Kusunoki M, Goldberg ME. The representation of visual salience in monkey parietal cortex. *Nature* 391: 481–484, 1998.

Gottlieb J, Kusunoki M, Goldberg ME. Simultaneous representation of saccade targets and visual onsets in monkey lateral intraparietal area. *Cereb Cortex* 15: 1198–1206, 2005.

Hanes DP, Schall JD. Neural control of voluntary movement initiation. *Science* 274: 427–430, 1996.

Huk AC, Shadlen MN. Neural activity in macaque parietal cortex reflects temporal integration of visual motion signals during perceptual decision making. *J Neurosci* 25: 10420–10436, 2005.

Mazurek ME, Roitman JD, Ditterich J, Shadlen MN. A role for neural integrators in perceptual decision making. *Cereb Cortex* 13: 1257–1269, 2003.

Mazzoni P, Bracewell RM, Barash S, Andersen RA. Motor intention activity in the Macaque's lateral intraparietal area. I. Dissociation of motor plan from sensory memory. *J Neurophysiol* 76: 1439–1456, 1996.

Mountcastle VB, Lynch JC, Georgopoulos A, Sakata H, Acuna C. Posterior parietal association cortex of monkey - command functions for operations within extrapersonal space. *J Neurophysiol* 38: 871–908, 1975.

Munoz DP, Wurtz RH. Saccade-related activity in monkey superior colliculus. I. Characteristics of burst and buildup cells. *J Neurophysiol* 73: 2313–2333, 1995.

Newsome WT, Britten KH, Movshon JA, Shadlen MN. Single neurons and the perception of visual motion. In: *Neural Mechanisms of Visual Perception: Proceedings of the Retina Research Foundation Symposium*, edited by Lam DMK, Gilbert C. The Woodlands, TX: Portfolio Publishing, 1989.

Oristaglio J, Schneider DM, Balan PF, Gottlieb J. Integration of visuospatial and effector information during symbolically cued limb movements in monkey lateral intraparietal area. *J Neurosci* 26: 8310–8319, 2006.

Platt ML, Glimcher PW. Responses of intraparietal neurons to saccadic targets and visual distractors. *J Neurophysiol* 78: 1574–1589, 1997.

Platt ML, Glimcher PW. Neural correlates of decision variables in parietal cortex. *Nature* 400: 233–238, 1999.

Robinson DL, Goldberg ME, Stanton GB. Parietal association cortex in primate - sensory mechanisms and behavioral modulations. *J Neurophysiol* 41: 910–932, 1978.

Roitman JD, Shadlen MN. Response of neurons in the lateral intraparietal area during a combined visual discrimination reaction time task. *J Neurosci* 22: 9475–9489, 2002.

Russ BE, Kim AM, Abrahamsen KL, Kiringoda R, Cohen YE. Responses of neurons in the lateral intraparietal area to central visual cues. *Exp Brain Res* 174: 712–727, 2006.

Shadlen MN, Gold JI. The neurophysiology of decision-making as a window on cognition. In: *The Cognitive Neurosciences*, edited by Gazzaniga MS. Cambridge, MA: MIT Press, 2004, p. 1229–1241.

Shadlen MN, Newsome WT. Motion perception: seeing and deciding. *Proc Natl Acad Sci USA* 93: 628–633, 1996.

Shadlen MN, Newsome WT. Neural basis of a perceptual decision in the parietal cortex (area LIP) of the rhesus monkey. *J Neurophysiol* 86: 1916–1936, 2001.

Smith PL, Ratcliff R. Psychology and neurobiology of simple decisions. *Trends Neurosci* 27: 161–168, 2004.

Snyder LH, Batista AP, Andersen RA. Coding of intention in the posterior parietal cortex. *Nature* 386: 167–170, 1997.

Sugrue LP, Corrado GS, Newsome WT. Matching behavior and the representation of value in the parietal cortex. *Science* 304: 1782–1787, 2004.

Zhang J, Riehle A, Requin J. Analyzing neuronal processing locus in stimulus-response association tasks. *J Math Psychol* 41: 219–236, 1997a.

Zhang J, Riehle A, Requin J, Kornblum S. Dynamics of single neuron activity in monkey primary motor cortex related to sensorimotor transformation. *J Neurosci* 17: 2227–2246, 1997b.

Zhang M, Barash S. Neuronal switching of sensorimotor transformations for antisaccades. *Nature* 408: 971–975, 2000.

Zhang MS, Barash S. Persistent LIP activity in memory antisaccades: working memory for a sensorimotor transformation. *J Neurophysiol* 91: 1424–1441, 2004.